

# Column dampers with negative stiffness: high damping at small amplitude

adapted from Kalathur, H., Lakes, R. S., Column dampers with negative stiffness: high damping at small amplitude, *Smart Materials and Structures*, 22, 084013 (8pp) (2013)

H Kalathur<sup>1,2</sup>, R S Lakes<sup>1,2,3</sup>

<sup>1</sup>Engineering Mechanics Program, University of Wisconsin-Madison, WI, 53706 USA

<sup>2</sup>Engineering Physics, University of Wisconsin-Madison, WI, 53706 USA

E-mail: <sup>3</sup>[lakes@engr.wisc.edu](mailto:lakes@engr.wisc.edu)

**Abstract:** High structural damping combined with high initial stiffness is achieved at small amplitude via negative stiffness elements. These elements consist of columns in the vicinity of post-buckling transition between contact of flat surfaces and edges of the ends for which negative incremental structural stiffness occurs. The column configuration provides high initial structural stiffness equal to the intrinsic stiffness of the column material. Columns of polymers polymethyl methacrylate (PMMA) and polycarbonate were used. By tuning of pre-strain, a very high mechanical damping, was achieved for small amplitude oscillations. The product of effective stiffness and effective damping as a figure of merit  $|E_{\text{eff}}|\tan \delta_{\text{eff}}$  of about 1.5 GPa was achieved for polymer column dampers in the linear domain and about 1.62 GPa in the small amplitude nonlinear domain. For most materials this value generally never exceeds 0.6 GPa.

## 1. Introduction

A combination of stiffness and viscoelastic damping is desirable for applications such as reduction of noise and vibration in machinery and vehicles. Structural materials such as steel, brass, and aluminum alloys are stiff but have low damping:  $\tan \delta$  is typically  $10^{-6}$  to  $10^{-4}$ . The loss tangent  $\tan \delta$  is a measure of damping. The loss angle  $\delta$  is the phase angle between stress and strain sinusoids.  $\tan \delta$  is proportional to the energy loss per cycle within linear viscoelasticity. Polymer damping layers have higher damping  $\tan \delta$  of 0.1 to 1 but they are not stiff; also they are highly temperature dependent.

High damping can be attained via choice or design of materials or via negative stiffness. Negative structural stiffness entails a reaction force in the same direction as the displacement. Such a condition is unstable unless it is constrained.

Negative stiffness can be attained in a variety of ways. For example a slender bar in a post-buckled 'S' shaped configuration is a lumped structural system in unstable equilibrium (Bazant and Cedolin, 1991). If the bar is constrained laterally, it may be stabilized and the negative stiffness measured. Structures containing buckled tubes (Lakes 2001a) exhibit negative stiffness that is observed experimentally under displacement control as a constraint. These structures exhibit extremely high structural damping under small oscillations following tuning of the pre-strain. The high damping is understood in the context of composite theory of Reuss (series) systems (Lakes 2001a). Specifically, one allows one modulus in the Reuss formula to become negative; the moduli become complex to allow viscoelastic behavior. As modulus is tuned, damping, considered as the ratio of imaginary to real part of the composite modulus, becomes singular. As a further example of a lumped (structural) system, envisage as a set of linear elastic springs having positive stiffness. The geometry is shown below in figure 1. In the unstretched configuration, figure 1(a), the force displacement relationship has positive slope, hence positive stiffness. Negative stiffness can now be attained by

displacing the point a to the right compressing the springs to reach the configuration shown in figure 1(b). If the stiffness  $k_2$  is small, the configuration is unstable, as a slight perturbation would cause the structure to snap-through, figure 1(c). Also, a flexible tetrakaidecahedron as a model of a foam cell, exhibits a force-displacement relationship that is not monotonic, so there is negative stiffness over a range of strain (Lakes 2001a).

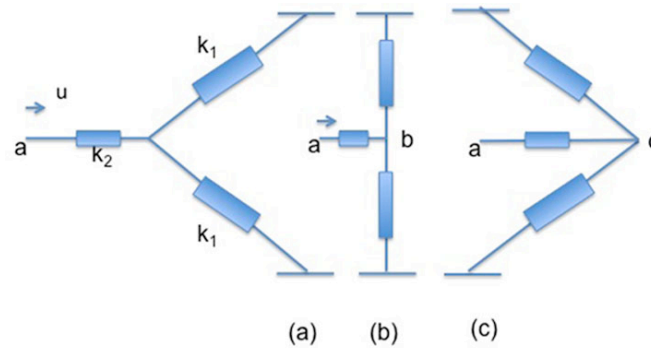


**Figure 1:** Geometry of linear elastic springs demonstrating negative stiffness in a lumped system. Force or displacement is applied at the left, at point a. (adapted from Jaglinski 2005)

- (a) The springs are unstretched (b) The springs are pre-loaded; this is unstable unless constrained.  
(c) Snap-through to a new stable configuration.

Negative stiffness (modulus) (Wang and Lakes 2004) can also occur in *distributed* systems, i. e. materials. Continuum elasticity theory defines modulus as the ratio of the stress to the strain. However, negative stiffness in this context must not be confused with negative Poisson's ratio (Lakes 2001b). Poisson's ratio,  $\nu$ , is defined as the negative transverse strain divided by the longitudinal strain, of an object subject to unidirectional stress. For most solids,  $\nu$  has values between 0.25 and 0.33. The allowable range of Poisson's ratio,  $-1 < \nu < 0.5$ , corresponds to the requirement for an unconstrained block of material to have positive moduli for stability. Poisson's ratio as small as  $-0.7$  obtained in foams (Lakes 1987) is stable. Bounds on the elastic properties of heterogeneous materials have been derived based on positive definite strain energy (Hashin and Shtrikman, 1962), which entails positive phase properties. Therefore they do not apply to materials or systems with constituents of negative stiffness. The formulas for modulus or damping provided by the bounds can be exceeded (Lakes 2001b) if negative stiffness is incorporated. Bounds on viscoelastic properties are also known (Gibiansky and Milton, 1993) but negative stiffness was not considered. Materials with negative moduli can be stabilized by a constraint, as by the matrix of a composite. This has allowed extremely high values of physical properties to be attained in the laboratory (Lakes et al. 2001c; Jaglinski et al. 2007).

The above methods to obtain negative structural stiffness in *lumped* systems also entail substantial compliance. To achieve high initial stiffness, a column design was developed to provide hysteresis in the post-buckling regime. Post-buckling theory for elastic structures deals with the shape of the load-deformation curve after initial instability (Budiansky, 1974). Tube buckling gives rise to decreasing force with increasing deformation (Bazant and Cedolin 1991). Columns in which the ends tilt during buckling and post-buckling also exhibit negative stiffness: decreasing force with increasing deformation. Buckling of viscoelastic columns is well known (Hilton, 1952; Libove, 1952); most analyses deal with performance of the columns as structural supports. For example, if the material is linear and its creep has an asymptote there will be a safe load below which no buckling occurs (Vinogradov, 1987). Divergence occurs in a finite time for a nonlinearly viscoelastic metal (Libove, 1952).

Columns prior to buckling exhibit the same initial stiffness as the parent material in contrast to beam bend models; high stiffness is beneficial in some damping applications. Previous column based high performance dampers based on lumped negative stiffness systems (Dong and Lakes 2012) involved relatively large amplitude oscillations. For some applications, high damping of small amplitude oscillations allowed is essential. In the present research, design considerations for column based dampers for small amplitude are developed, specifically in the linear regime and in the nonlinear regime at strains comparable to working strain in high damping metals.

## 2. Methods

Commercial, extruded PMMA rods (McMaster-Carr, #8531K13) were used for the purpose of this work. Columns of lengths of about 200mm and 122mm were cut using a band saw (Pro-Tech 3203). The ends of these columns were ground using 600C grade abrasive paper to ensure flat surfaces. A digital caliper was used to determine the lengths and the diameter of the columns. For each aspect ratio (d/L), two columns were tested in which one of the columns had the ends glued (Loctite instant adhesive) to the test frame (platens/grips), thus achieving a built-in condition (figure 2). The glue is a polymer of stiffness comparable to the column; moreover a thin layer was used. Therefore glue compliance is not likely to cause significant deviation from the ideal built in condition.

The results obtained in this endeavor were based on the analysis of force-displacement relationship when the columns were subjected to cyclic compression at ambient temperature. The relationship was obtained using a 90 kN capacity servo-hydraulic test frame (MTS corp. Minneapolis, MN), a digital oscilloscope (Tektronix, TDS 3012, 2 channel, 100MHz, 1.25GS/s) and a lock-in amplifier (Ithaco-NF, type 3961B, 2 phase). The digital oscilloscope was used to examine the Lissajous figure, that is the force-displacement plot. The MTS test frame was operated under displacement control with 1 Hz sinusoidal input; an amplified scale of 9 kN maximum was used to improve resolution of force. For sufficiently small amplitude, the response was determined to be linear by the elliptic shape of the load-deformation curve (Lissajous figure). To eliminate noise at small amplitude, the lock in amplifier was used to measure the phase shift  $\phi$  between displacement and force waveforms and to eliminate the noise associated with small signals. The structural phase shift  $\phi$  is identical to the material phase shift  $\delta$  when the column is straight in which case the structural stiffness relates simply to the material Young's modulus. Therefore the damping ( $\tan \phi$ ) determined this way is a true  $\tan \phi$ , not an effective one that is obtained for a nonlinear system. Response to small amplitude input was determined with the lock in amplifier in the linear regime and with the digital oscilloscope in the nonlinear regime. The damping for non-linear Lissajous figure was determined by comparing the area ratio (and in turn the mass ratio of the area) with that of an elliptic Lissajous figure of known phase lag (1 radian), within the same rectangular force-displacement boundaries. This provides a specific damping capacity  $\Psi$  presented as effective damping  $\tan \phi_{\text{eff}} = \Psi/2\pi$ . Symbolically, the effective damping was obtained as follows.

$$\frac{A_1}{A_2} = \frac{m_1}{m_2} = \frac{\tan \phi_1}{\tan \phi_2}$$

where,

$A_1$  is the area of the elliptic lissajous figure corresponding to  $\phi_1 = 1$  radian

$m_1$  is the mass of the elliptic lissajous figure corresponding to  $\phi_1 = 1$  radian

$A_2$  is the area of the lissajous figure to be determined and corresponding to  $\phi_2$

$m_2$  is the mass of the lissajous figure to be determined and corresponding to  $\phi_2$

Each column was secured between the platens by moving the grips on the servo- hydraulic frame towards each other until contact. This caused a slight pre-load (about 9-18 N) to be applied on the column for ensuring proper contact. In the case of glued end condition, the adhesive was applied to the end surfaces and the platens were moved towards each other until the column was secured between them.

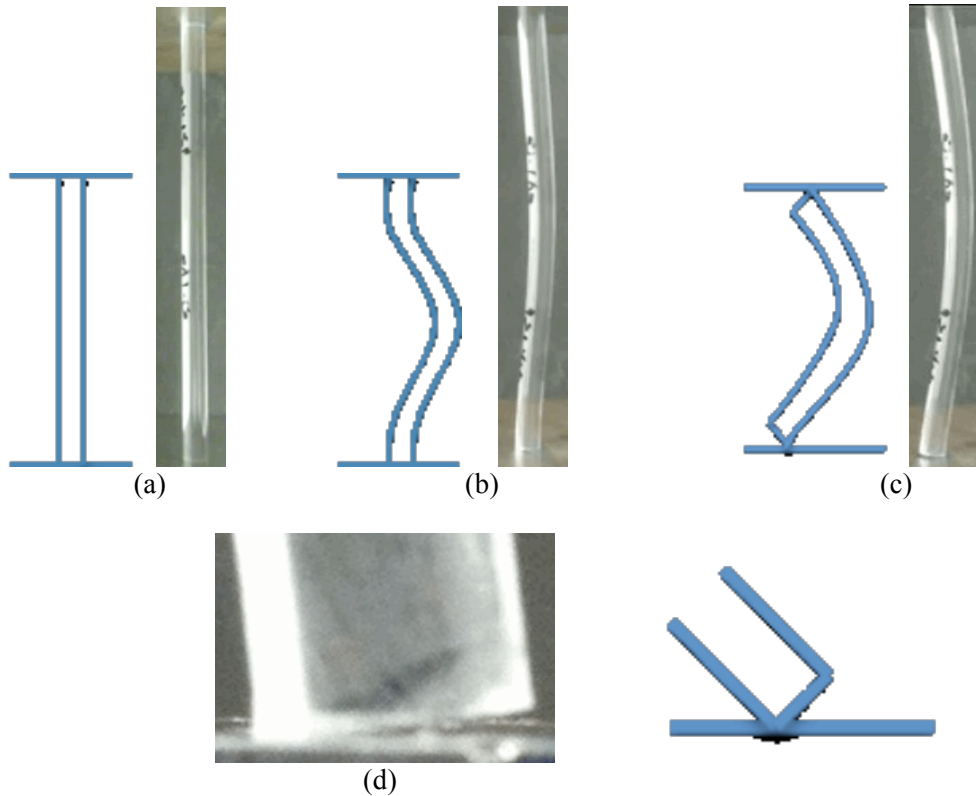
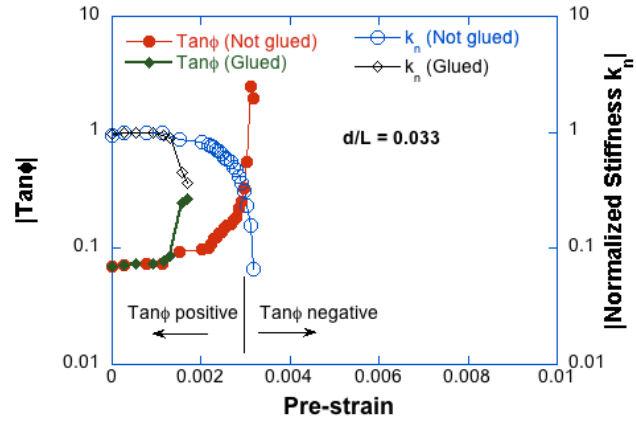


**Figure 2:** (a) Experimental set up showing the column secured between the platens. (b) Initial deflection similar to clamped ends column. (c) Column end tilt for the case of ends not glued. (d) Column end tilt in close-up. Diagrams of the geometry for (a), (b) and (c) are also shown.

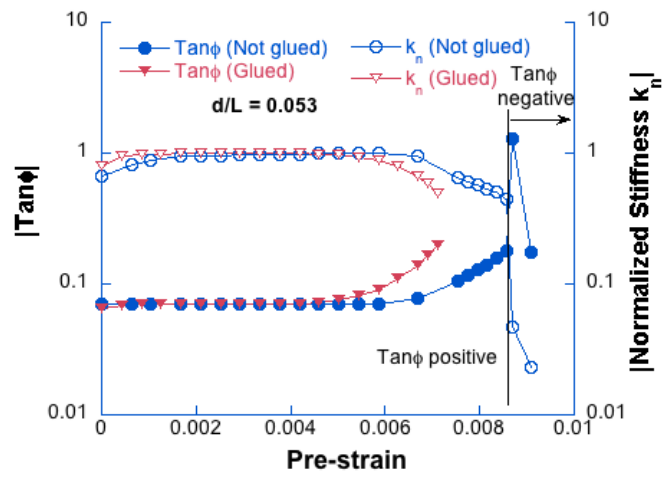
### 3. Results and Discussion

#### 3.1. Small deformation, linear

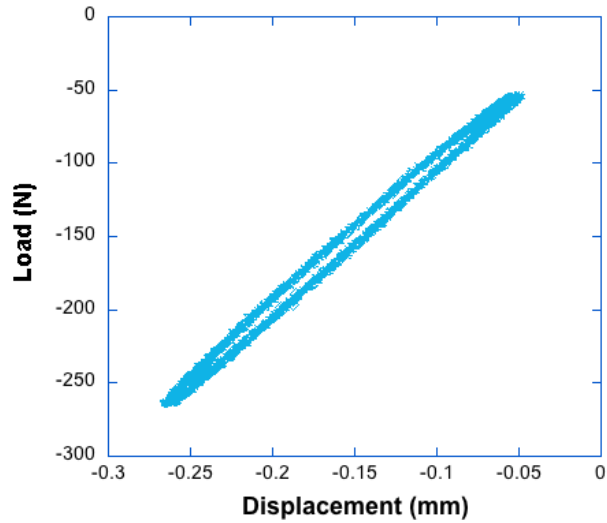
The plots below (figure 3) show the stiffness and damping dependence on pre-strain, for aspect ratios 0.033 and 0.053. At zero pre-strain, the damping approaches the intrinsic value,  $\tan \phi = 0.07$  for PMMA at 1 Hz. Figure 3(c) shows a typical elliptical Lissajous figure when the column is straight, i.e. in the linear range.



(a)



(b)



(c)

**Figure 3:** PMMA columns at 1Hz for (a)  $d/L=0.033$  and (b)  $d/L=0.053$ . The high damping occurs only when the end contact condition changes from flat surface contact to edge contact, indicating a negative incremental stiffness. (c) Elliptic Lissajous figure of a PMMA column,  $d/L=0.033$ .

The damping attains a large value only when the ends of the columns are allowed to tilt, indicating a negative incremental stiffness. The normalization of stiffness is with respect to the stiffness when the column is straight. Negative phase angle occurs in this regime. That does not entail energy gain because the stiffness is negative as well (Lakes 2001a). The imaginary part of the complex stiffness is still positive, in keeping with a passive system (Christensen, 1972). The abrupt rise in phase angle and compliance in figure 3 resembles a resonance. The resemblance is formal only. The equation governing the stiffness of a system containing negative stiffness resembles that of a resonance. It is not resonant since the opposing terms in the denominator arise from static stiffness without inertia (Lakes, 2001a, b).

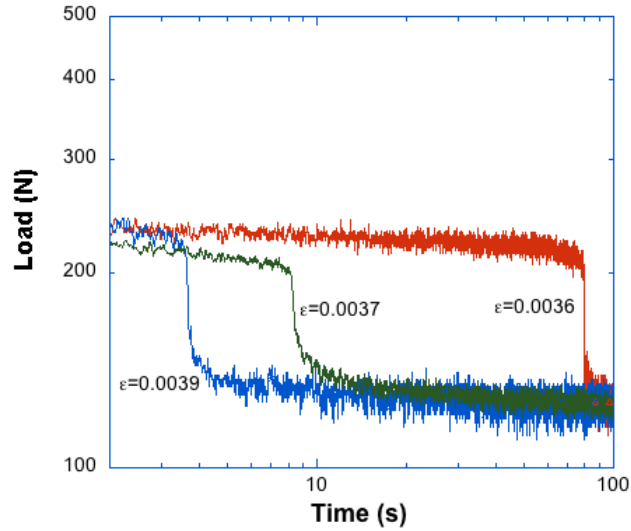


**Figure 4:** Relaxation of PMMA column at different compressive strains imposed as a step function in time. As the strain gets closer to the transition, the snap occurs faster. Farther away from the transition strain, it takes longer to snap.

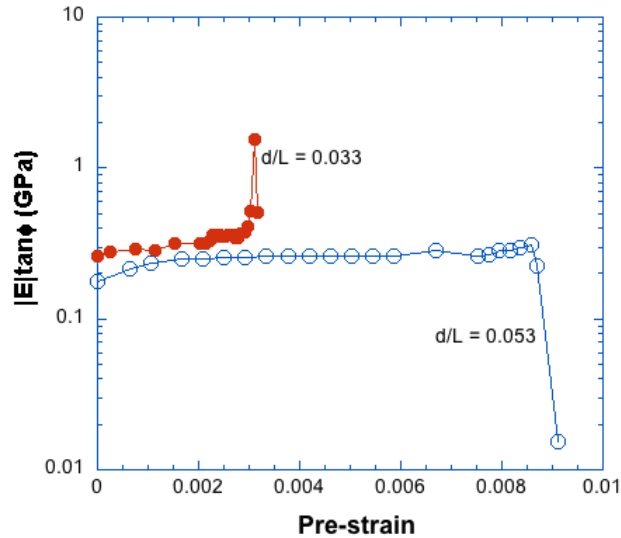


**Figure 5:** Product of effective modulus and damping, at 1 Hz versus pre-strain.

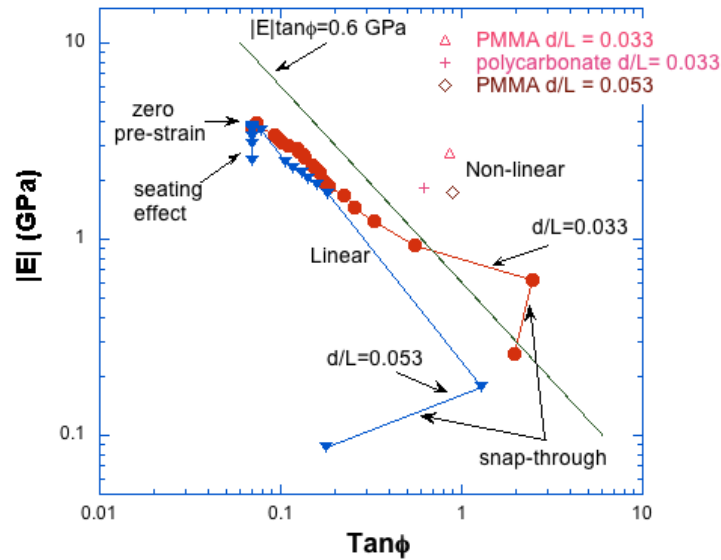


**Figure 6:** Stiffness-loss map of PMMA column, at 1 Hz in the linear regime. Also included are the results corresponding to the non-linear, small deformation regime. Results for non-linear hysteresis are for PMMA with  $d/L=0.053$  and  $d/L=0.033$ , and for polycarbonate with  $d/L = 0.033$ . The tuning variable is pre-strain. The figure of merit for non-linear exceeded 0.6 GPa for both PMMA and polycarbonate, well above the typical maximum value for materials.

The stiffness-loss map was generated using the data from figures 3a and 3b, except that now the stiffness is plotted vs.  $\tan \phi$ , instead of pre-strain. The tuning variable is still pre-strain. The red circles and blue triangles are the results for  $d/L=0.033$  and  $d/L=0.053$  respectively as indicated in the figure by arrows.

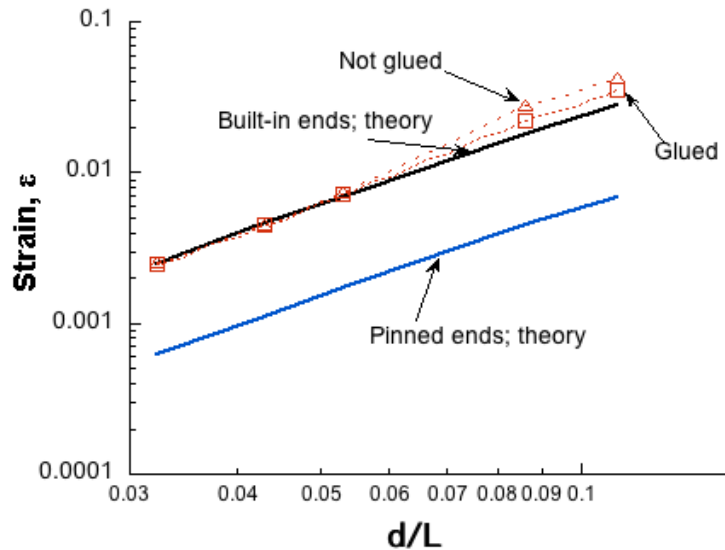


**Figure 7:** Strain thresholds for buckling of PMMA columns for several aspect ratios; comparison of theory and experiment.

Figure 7 shows the buckling thresholds for conditions in which the ends are glued and not glued based on a criterion of 5% softening of the effective stiffness, or the deviation of the load-displacement curve from the initial linear portion by 5%. Doing this accounted for the noise level that was present in the load channel of the test frame. The experimental results agree well with theoretical values, as shown in the plot. Gluing the ends of the column generated the built-in condition effectively. The thresholds for the theoretical built-in (clamped) and pinned ends were obtained using the Euler's buckling equation wherein the modulus E was divided out to calculate the strain.

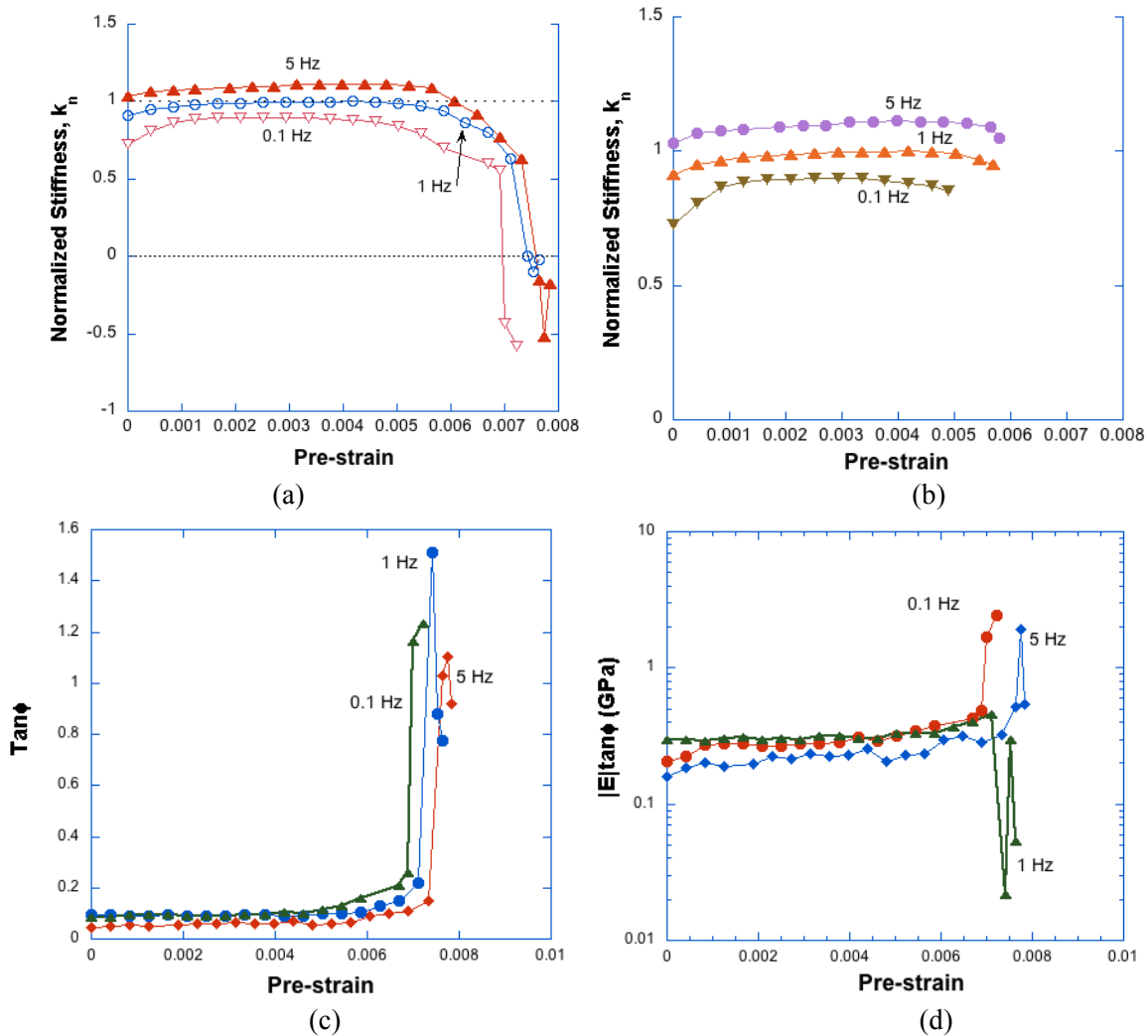


**Figure 8:** (a). Stiffness response to linear range small oscillations performed with PMMA columns 121.4mm long 6.453mm diameter, at 0.1Hz, 1Hz and 5Hz. The material behaves stiffer at higher frequencies. (b) Stiffness roll off at each frequency based on 5% softening. This plot is obtained by truncating the post softening behavior, for 0.1Hz, 1Hz and 5Hz, in (a). (c) Damping response to linear range small oscillations. The high damping occurs only when the end contact condition changes from flat surface contact to edge contact, indicating a negative incremental stiffness. (d) The figure of merit,  $|E|\tan \phi$  is plotted versus pre-strain at 0.1Hz, 1Hz and 5Hz. It was possible to achieve  $|E|\tan \phi \sim 2.5$  GPa at 0.1Hz and about 1.9 GPa at 5Hz, well above the typical maximum value for materials.

Frequency dependence as well as pre-strain dependence of effective structural stiffness and damping is shown in figure 8. The normalization of stiffness is with respect to the stiffness when the column is

straight. At higher frequencies (figure 8), columns appear stiffer due to viscoelastic effects. The transition to the buckled state occurs sooner (less pre-strain) at lower frequency than at a higher frequency. Large  $\tan \phi$  occurs under small amplitude provided one tunes the system near the threshold for snap through buckling. As in Figure 3, the variation in damping and compliance near the buckling threshold is not due to resonance. In the experiments, a change in frequency gives rise to a slight shift from the material viscoelasticity, much smaller than the shift that would be expected from inertial effects.

### 3.2. Small deformation, nonlinear

The plots in figure 9 show the non-linear hysteresis at small deformation amplitude of PMMA columns with aspect ratios 0.033 and 0.053. In each case, the peak-peak displacement amplitude along with pre-strain was chosen to be sufficient to capture the linear, snap-through and post snap through effects. The linear portion of the curve is truncated due to pre-strain. The initial stiffness of the column is equal to the Young's Modulus of the parent material PMMA, which is about 3 GPa (not shown in figure 9) based on the initial slope of the Lissajous figure. Figure 10 shows a comparison between columns of two polymers, PMMA and polycarbonate. Polycarbonate has a lower intrinsic damping, about 0.003, in comparison with PMMA, about 0.07 at 1 Hz. Both columns exhibit similar hysteresis associated with buckling, but the transition is sharper in the case of polycarbonate.

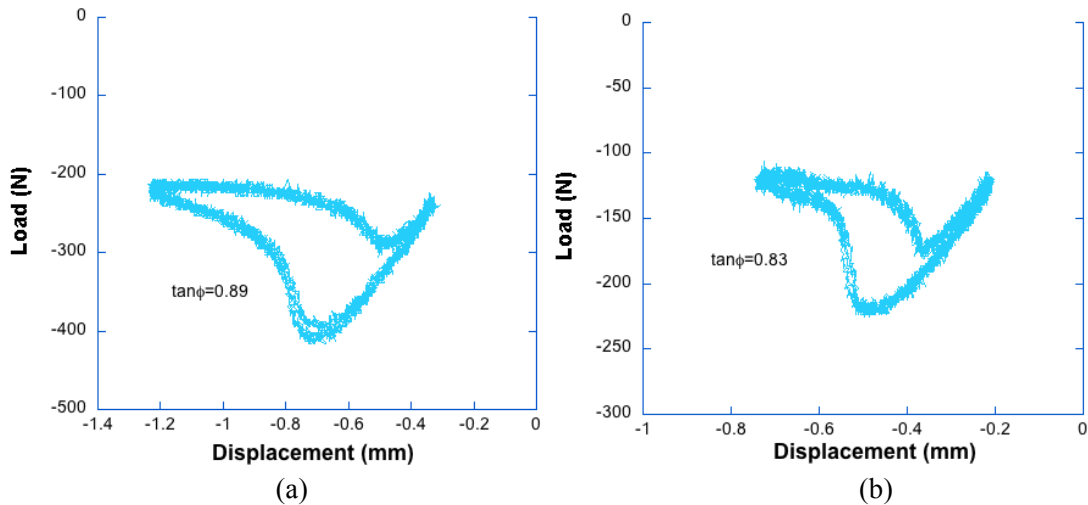


**Figure 9:** (a) Non-linear hysteresis of PMMA column with  $d/L=0.053$ . The peak to peak displacement amplitude is 0.89mm and column length is 121.4mm. (b) Non-linear hysteresis of PMMA column with  $d/L=0.033$ . The peak to peak displacement amplitude is 0.53mm and column length is 197.6mm.

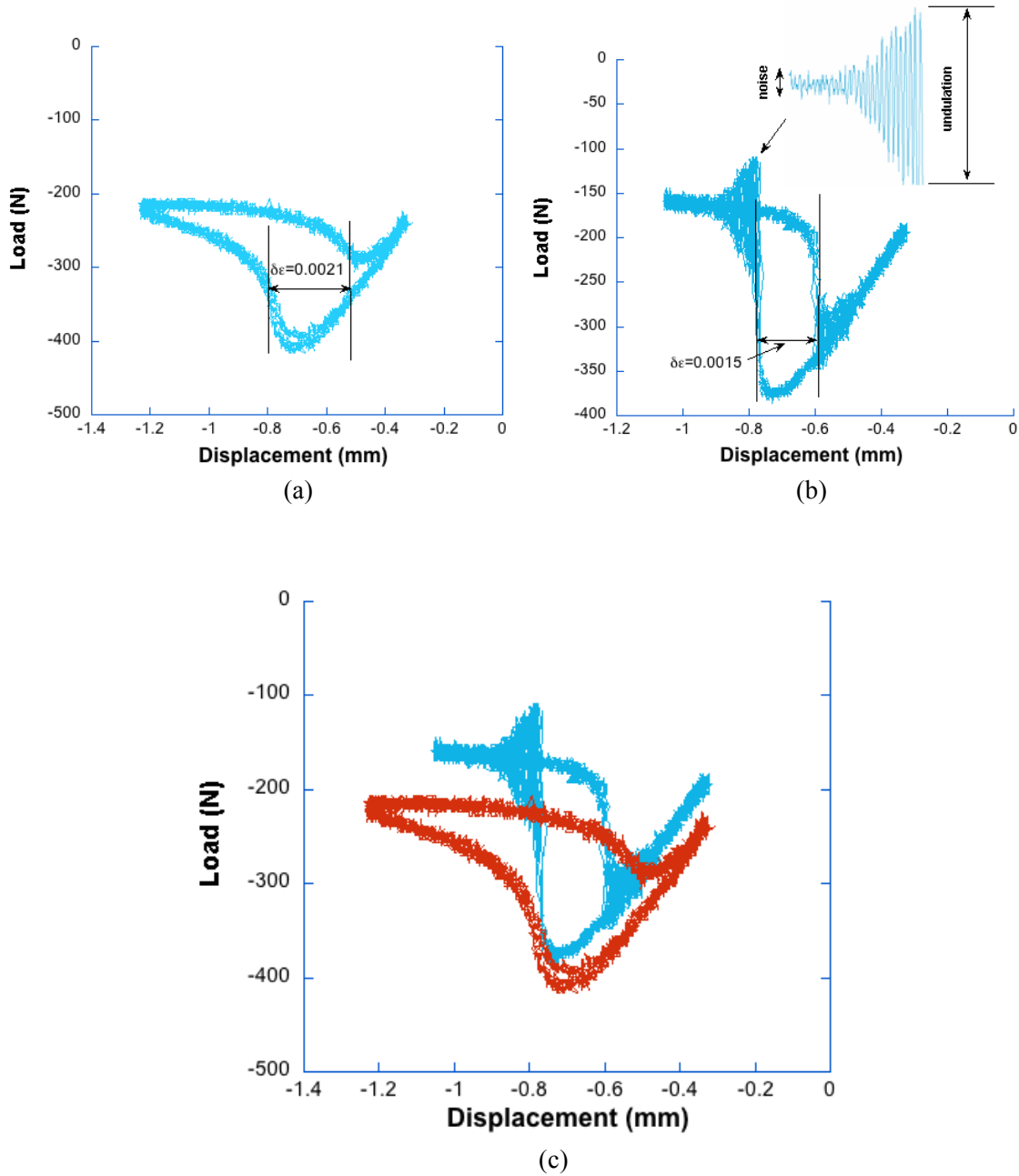


**Figure 10:** (a) Non-linear small strain hysteresis of PMMA column with  $d/L=0.053$ . The peak to peak displacement amplitude is 0.89mm and column length is 121.4mm. (b) Non-linear small strain hysteresis of polycarbonate column with  $d/L=0.053$ . The peak to peak displacement amplitude is 0.77mm and column length is 121.4mm. (c) figures (a) and (b) overlaid in a single plot. The snap through in the case of polycarbonate is much more sharp in comparison to PMMA because of the low intrinsic damping of polycarbonate and hence some undulation can be seen just after snap-through for polycarbonate. The undulation (inset of figure 10b) should not be confused with the noise that is present in the data, which is about  $\pm 5.8\text{N}$  in the load channel.

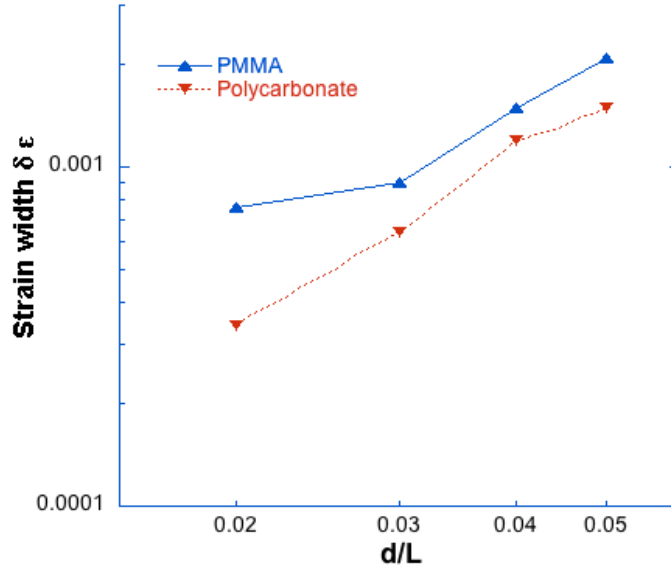


**Figure 11:** Width of small strain nonlinear hysteresis is plotted versus aspect ratio. The frequency is 1 Hz. The behavior of PMMA is compared with that of polycarbonate.

The width of hysteresis was determined by determining the increment of strain between inflection points in the hysteresis curve as shown in figure 10. This strain width (figure 11) reveals an increasing trend with aspect ratio. In case of polycarbonate, the snap-through was very sharp in comparison to PMMA, because of lower intrinsic damping of polycarbonate, but the dependence of width on aspect ratio is similar. It is possible to tune the system around just the hysteresis portion and not including the initial linear portion and the post snap portion. This way, an even higher damping (up to  $\tan \phi = 2$ ) could be achieved.

Nonlinear damping in the small strain regime is similar to the hysteresis (Dong and Lakes, 2012) seen at higher strains (0.002 to 0.025). At such high strains, metallic damping materials will suffer yield. Nonlinear damping in the small strain regime below 0.001 is potentially useful because nonlinear materials are used at such strains. With appropriate pre-strain, column based dampers can attain extreme high damping combined with the initial stiffness of the column material without use of special materials. For example a damper module based on steel or graphite-epoxy composite can provide high stiffness combined with high effective damping. The strain level of operation can be made to match that of copper manganese alloys used in naval ship propellers. Such alloys are considered to be high damping metals. These alloys exhibit damping of about 0.003 or less at small strains below  $10^{-5}$  but can exceed a damping of 0.01 at a few Hz if the strain is sufficiently large,  $3 \times 10^{-4}$  [Laddha and Van Aken 1995].

Experimentally the range of aspect ratio was limited by the following. Higher aspect ratios correspond to short specimens; if too short they may yield or break. Lower aspect ratios of constant diameter correspond to longer specimens; if too long, they exceed the available length space in the test frame.

Design considerations for structural dampers suitable for small amplitude input are as follows. To achieve stability, the buckled columns must be constrained. In the present results, constraint was achieved in the test frame via displacement control. Constraint can also be achieved by incorporating one or more buckled columns in a module stabilized by shorter or thicker columns that do not buckle as was done by (Dong and Lakes 2012). Attainment of high damping in the linear regime requires tuning of pre-strain close to a threshold of instability. That threshold is influenced by time dependent

relaxation. The delicacy of tuning could be ameliorated by using an array of columns cut to different length to obtain a range of buckling thresholds; there would be a corresponding penalty in maximum damping. Small amplitude oscillations can also be heavily damped by buckled columns via nonlinear hysteresis. The strain range can be comparable to that associated with use of nonlinear high damping metals such as copper manganese alloys. Use of appropriate pre-strain allows extremely high damping 100 times the value attainable with these alloys.

#### **4. Conclusions**

Negative stiffness allows for high damping. The initial stiffness of the column is equal to the Young's Modulus of the parent material PMMA, which is about 3 GPa (not shown in figure 9) based on the initial slope of the Lissajous figure. This is in contrast to "S" shaped bent beams or a kinked tube which are compliant. Columns with ends free to tilt provide high initial stiffness and they exhibit the capability of snap-through hysteresis and high damping of small amplitude oscillations.

The  $\tan \phi$  exceeds 2.4 in a tuned polymer damper, much larger than the value of 0.07 associated with the intrinsic damping of PMMA. The effective modulus -  $\tan \phi$  product exceeds 0.6 GPa in tuned linear dampers.

#### **Acknowledgement**

We acknowledge DARPA under the direction of Judah Goldwasser for funding this project.

## References

- Bazant Z and Cedolin L 1991, *Stability of Structures* (Oxford University Press, Oxford).
- Budiansky B 1974, Theory of Buckling and Post-Buckling Behavior of Elastic Structures, *Advances in Applied Mechanics*, Vol. 14, 1-65.
- Christensen R M 1972, Restrictions Upon Viscoelastic Relaxation Functions and Complex Moduli, *Journal of Rheology*, Vol. 16, Issue 4, pp. 603-614.
- Dong L and Lakes R S 2012, Advanced Damper with Negative Structural Stiffness Elements, *Smart Materials and Structures*, Vol. 21, 075026, 17 pp. .
- Gibiansky L V and Milton G W 1993, On the Effective Viscoelastic Moduli of Two-Phase Media. I. Rigorous Bounds on the Complex Bulk Modulus, *Mathematical and Physical Sciences*, Vol. 440, No. 1908, pp. 163-188.
- Hashin Z and Shtrikman S 1962, On Some Variational Principles in Anisotropic and Non-homogenous Elasticity, *Journal of Mechanics and Physics of Solids*, Volume 10, Issue 4, pages 335-342.
- Hilton H H 1952, Creep Collapse of Viscoelastic Columns with Initial Curvatures, *Journal of the Aeronautical Sciences* (Institute of the Aeronautical Sciences), Vol. 19, No. 12, pp. 844-846.
- Jaglinski T, Stone D and Lakes R S 2005, Internal Friction Study of a Composite with a Negative Stiffness Constituent, *Journal of Materials Research*, Vol. 20, Number 9, pp. 2523-2533.
- Jaglinski T, Stone D S, Kochmann D, and Lakes R S 2007, Materials with Viscoelastic Stiffness Greater than Diamond, *Science*, 315, 620-622.
- Laddha S and Van Aken D C 1995, On the Application of Magnetomechanical Models to Explain Damping in an Antiferromagnetic Copper-manganese alloy, *Metall. and Materials Trans.* 26A, 957-964.
- Lakes R S 1987, Foam Structures with a Negative Poisson's ratio, *Science*, 235 1038-1040.
- Lakes R S 2001 (a), Extreme Damping in Compliant Composites with a Negative Stiffness Phase, *Philosophical Magazine Letters*, Vol. 81, Number 2, 95-100.
- Lakes R S 2001 (b), Extreme Damping in Composite Materials with a Negative Stiffness Phase, *Physical Review Letters*, Vol. 86, Number 13, pp. 2897-2900.
- Lakes RS, Lee T, Bersie A and Wang Y C March 2001 (c), Extreme Damping in Composite Materials with Negative Stiffness Inclusions, *Nature*, Vol. 410, 565-567.
- Libove C 1952, Creep Buckling of Columns, *Journal of the Aeronautical Sciences* (Institute of the Aeronautical Sciences), Vol. 19, No. 7, pp. 459-467.
- Vinogradov A M 1987, Buckling of Viscoelastic Beam Columns, *AIAA journal*, Volume 26, No. 3, pp. 479-483.

Wang Y C and Lakes R S 2004, Extreme Stiffness Systems due to Negative Stiffness Elements, *Am. J. Phys.*, 72 (1), pp.40-50.